Speckle Suppression Method in SAR Image Based on Curvelet Domain BivaShrink Model

Wenbo Wang
College of Science, Wuhan University of Science and Technology, Wuhan,430065, China
Email: articlewwb@yahoo.com.cn

Xiaodong Zhang
State Key Laboratory of Information Engineering in Surveying Mapping and Remote Sensing, Wuhan, 430072, China
State Key Laboratory of Satellite Ocean Environment Dynamics,Second Institute of Oceanography State Oceanic Administration, Hangzhou, China
Email: zxdlmars@whu.edu.cn

Xiangli Wang
School of Computer Science and Technology, Wuhan University of Technology, Wuhan 430063,China
Email: wangxiangli@whut.edu.cn

***Abstract*— Based on the statistical property of SAR image speckle noise and the property that the multiscale geometric analysis can capture the intrinsic geometrical structure of image, combining curvelet transform with BivaShrink denoising model, a method of SAR image denoising based on curvelet domain is presented in this paper. According to calculation of variance homogeneous measurement and curvelet coefficients of current layer and its parent layer, the local adaptive window is determined to optimally estimate shrinkage factor. The method can effectively reduce SAR speckle noise and preserving details of SAR image well through the correlation of curvelet coefficients in the same direction of subband and parent-layer subband. The experimental results show the presented method greatly improves the subjective visual effect and the numerical indicators of the denoised image.**

***Index Terms*— Curvelet transform, Variance homogeneous measurement, speckle suppression, SAR image**

I. INTRODUCTION

A Synthetic aperture radar (SAR) is an active microwave remote sensor. It can form an image at anytime and any weather. But the visibility of SAR image greatly reduces due to its inherent speckle noise, it is a key issue to effectively remove the speckle noise in a SAR image. The speckle noise is usually expressed as the multiplicative noise model.

Wavelet transform can achieve a good denoising result for SAR owing to its good time-frequency representation properties[1,2,3,4]. Wavelet is the optimal base when it represents the objective function with point singularity, but it isn't the optimal when it represents the singularity of line and hyperplane. To overcome this limitation, Candès and Donoho propose curvelet transform[5]. It can detect the singularity of line and surface well, and effectively deal with line singularity of two-dimensional space. Strack[6] applies hard thresholding and curvelet transform to denoise image, and gets a good denoising result. But the hard thresholding mistakes part of the small signal coefficient values for noise figure. It will lose a lot of details and blur the edge and texture of image, especially SAR image with complex background and rich edges and texture details. Many experiments show that BivaShrink denoising based on wavelet domain, proposed by Sendur[7], can effectively remove noise, and has lower computational complexity. This method demands to estimate the noise variance σ_n of noisy image and the variance σ_X of original image. σ_n is estimated usually through the median estimation. After the determination of σ_n, the estimation of σ_X is very important.Because the coefficients between all adjacent layers show a weak correlation after the image is transformed by the orthogonal wavelet, the BivaShrink denoising method uses the neighborhood window to estimate σ_X . This window has the following two properties[8]: (1) It is a square window with unchanged size and shape; (2) It only considers the wavelet coefficients of the same sub-band, ignoring the impact of parent-layer coefficients on σ_X .

While wavelets are used to separate point singularities, second generation wavelets, e.g. curvelets, are more suitable for the extraction of two dimensional features, as they are able to describe image discontinuities along a smooth line (an edge) with a minimum number of coefficients. The elementary components are the so-called ridgelets – due to their appearance like a ridge – that can have different scales (equivalent to their length), directions and positions in the image. This enables a selection of two dimensional features to be suppressed

doi:10.4304/jsw.8.4.947-954

(assumed noise) or to be emphasized (structure) by manipulating the corresponding coefficient of each ridgelet. In the following a short overview to related work especially to the development of curvelets is given. Then, the curvelet representation is roughly explained and three applications are presented: image denoising, structure enhancement and change detection over the city center of Munich (imaged by TerraSAR-X in the high resolution spotlight mode and VV polarization). So this paper shows the potential of the curvelet transform for SAR image analysis.

The curvelet transform used in this approach has originally been developed by (Cand`es and Donoho, 1999) to describe an object with edges with a minimal number of coefficients in the continuous space. Much research work was done to examine the behaviour of curvelets, to transfer the definitions from the continuous to the discrete space and to accelerate the computing time so that digital image processing becomes feasible. Many applications in different scientific fields have been published so far, e.g. in geo- and astrophysics, that are summarized on the curvelet homepage (Demanet).

In this paper, the BivaShrink denoising is extended to curvelet domain. However, when SAR image is denoised in curvelet domain, if we directly adopt the method proposed by Sendur to estimate σ_X , the estimation accuracy will be severely affected.

Firstly, the size of the neighborhood window $N(i, j)$ has greater influence on the estimation of $\sigma_X(i, j)$ and the whole denoising results. The increment of window usually leads to the reduction of $\sigma_X(i, j)$, and vice versa. If the size of window is too large, the edges and texture details of the image can be better maintained, but much noise is mistaken for useful signal to preserve. Otherwise, if the size of window is too small, lots of edges and texture details are treated as noise to remove, which will blur the image. Because SAR image has complex background, rich texture and obviously different variance in different regions, it is very difficult to accurately estimate the value of σ_X through using the neighborhood window with fixed size in each layer.

Secondly, the curvelet transform isn't an orthogonal transform. It exists a high degree of redundancy, which is $16J+1$ (where J denotes the number of the decomposed layers). The curvelet coefficients between adjacent layers show a strong correlation. If the correlation is considered to estimate the variance σ_X in the BivaShrink denoising based on curvelet domain, which is bound to further reduce the error of σ_X .

To solve the above two problems, a curvelet domain BivaShrink denoising method based on region segmentation is proposed. It adaptively determine the shape and size of the neighborhood window through calculating the variance homogeneous measurement and the regional energy ratio. Simultaneously, it estimates the variance σ_X of the original image according to the statistical information of the intra and inter-layer coefficients. The experimental results indicate that the proposed method can better suppress the speckle noise of SAR image, and effectively maintain the details information of the edges and texture. The subjective visual effect and the numerical indicators of the denoised images are greatly improved.

II. IMPROVED CURVELET DOMAIN BIVASHRINK DENOISING ALGORITHM

A. Curvelet Transform Model

The new ridgelet and curvelet transforms were developed over several years in an attempt to break an inherent limit plaguing wavelet denoising of images. This limit arises from the well-known and frequently depicted fact that the two-dimensional (2-D) wavelet transform of images exhibits large wavelet coefficients even at fine scales, all along the important edges in the image, so that in a map of the large wavelet coefficients one sees the edges of the images repeated at scale after scale. While this effect is visually interesting, it means that many wavelet coefficients are required in order to reconstruct the edges in an image properly.With so many coefficients to estimate, denoising faces certain difficulties. There is, owing to well-known statistical principles, an imposing tradeoff between parsimony and accuracy which even in the best balancing leads to a relatively high mean squared error (MSE). While this tradeoff is intrinsic to wavelet methods. There are also various discrete ridgelet transforms based on ideas of frames and orthobases. For all of these notions, one has frame/basis elements localized near lines at all locations and orientations and ranging though a variety of scales (localization widths). It has been shown that for these schemes, simple thresholding of the discrete ridgelet transform provides near-optimal -term approximations to smooth functionswith discontinuities along lines. In short, discrete ridgelet representations solve the problem of sparse approximation to smooth objects with straight edges.

In image processing, edges are typically curved rather than straight and ridgelets alone cannot yield efficient representations. However at sufficiently fine scales, a curved edge is almost straight, and so to capture curved edges, one ought to be able to deploy ridgelets in a localized manner, at sufficiently fine scales. Two approaches to localization of ridgelets are possible.

A special member of this emerging family of multiscale geometric transforms is the curvelet transform which was developed in the last few years in an attempt to overcome inherent limitations of traditional multiscale representations such as wavelets. Conceptually, the curvelet transform is a multiscale pyramid with many directions and positions at each length scale, and needle-shaped elements at fine scales. This pyramid is nonstandard, however. Indeed, curvelets have useful geometric features that set them apart from wavelets and the likes. For instance, curvelets obey a parabolic scaling relation which says that at scale 2^{-j} , each element has an envelope which is aligned along a "ridge" of length $2^{\frac{-j}{2}}$

and width 2^{-j} . We postpone the mathematical treatment of the curvelet transform to Section 2, and focus instead on the reasons why one might care about this new transformation and by extension, why it might be important to develop accurate discrete curvelet transforms. Curvelets are interesting because they efficiently address very important problems where wavelet ideas are far from ideal. We give three examples:

1. Optimally sparse representation of objects with edges. Curvelets provide optimally sparse representations of objects which display curve-punctuated smoothness—smoothness except for discontinuity along a general curve with bounded curvature. Such representations are nearly as sparse as if the object were not singular and turn out to be far more sparse than the wavelet decomposition of the object.

This phenomenon has immediate applications in approximation theory and in statistical estimation. In approximation theory, let f_m be the m -term curvelet approximation (corresponding to the m largest coefficients in the curvelet series) to an object $f(x_1, x_2) \in L^2(R^2)$. Then the enhanced sparsity says that if the object f is singular along a generic smooth C^2 curve but otherwise smooth, the approximation error obeys

$$\| f - f_m \|_{L^2}^2 \le C \cdot (\log m)^3 \cdot m^{-2}$$

and is optimal in the sense that no other representation can yield a smaller asymptotic error with the same number of terms. The implication in statistics is that one can recover such objects from noisy data by simple curvelet shrinkage and obtain a Mean Squared Error (MSE) order of magnitude better than what is achieved by more traditional methods. In fact, the recovery is provably asymptotically near-optimal. The statistical optimality of the curvelet shrinkage extends to other situations involving indirect measurements as in a large class of ill-posed inverse problems .

2. Optimally sparse representation of wave propagators. Curvelets may also be a very significant tool for the analysis and the computation of partial differential equations. For example, a remarkable property is that curvelets faithfully model the geometry of wave propagation. Indeed, the action of the wave-group on a curvelet is well approximated by simply translating the center of the curvelet along the Hamiltonian flows. A physical interpretation of this result is that curvelets may be viewed as coherent waveforms with enough frequency localization so that they behave like waves but at the same time, with enough spatial localization so that they simultaneously behave like particles. This can be rigorously quantified. Consider a symmetric system of linear hyperbolic differential equations of the form

$$\frac{\partial u}{\partial t} + \sum_k A_k(x) \frac{\partial u}{\partial x_k} + B(x)u = 0$$

where u is an m -dimensional vector and $x \in R^n$. The matrices A_k and B may smoothly depend on the spatial variable x , and the A_k are symmetric. Let E_t be the solution operator mapping the wavefield $u(0, x)$ at time zero into the wavefield $u(t, x)$ at time t . Suppose that $\varphi(n)$ is a (vector-valued) tight frame of curvelets. Then [5] shows that the curvelet matrix

$$E_t(n, n') = < \varphi_n, E_t(\varphi_n') >$$

is sparse and well-organized. It is sparse in the sense that the matrix entries in an arbitrary row or column decay nearly exponentially fast (i.e., faster than any negative polynomial). And it is well-organized in the sense that the very few nonnegligible entries occur near a few shifted diagonals. Informally speaking, one can think of curvelets as near-eigenfunctions of the solution operator to a large class of hyperbolic differential equations. On the one hand, the enhanced sparsity simplifies mathematical analysis and allows to prove sharper inequalities. On the other hand, the enhanced sparsity of the solution operator in the curvelet domain allows the design of new numerical algorithms with far better asymptotic properties in terms of the number of computations required to achieve a given accuracy .

3. Optimal image reconstruction in severely ill-posed problems. Curvelets also have special microlocal features which make them especially adapted to certain reconstruction problems with missing data. For example, in many important medical applications, one wishes to reconstruct an object $f(x_1, x_2)$ from noisy and incomplete tomographic data, i.e., a subset of line integrals of f corrupted by additive moise modeling uncertainty in the measurements. Because of its relevance in biomedical imaging, this problem has been extensively studied (compare the vast literature on computed tomography). Yet, curvelets offer surprisingly new quantitative insights For example, a beautiful application of the phase-space localization of the curvelet transform allows a very precise description of those features of the object of f which can be reconstructed accurately from such data and how well, and of those features which cannot be recovered

$$f = \sum_{n \in good} < f, \varphi_n > \varphi_n + \sum_{n \notin good} < f, \varphi_n > \varphi_n$$

The first part of the expansion can be recovered accurately while the second part cannot. What is interesting here is that one can provably reconstruct the "recoverable" part with an accuracy similar to that one would achieve even if one had complete data. There is indeed a quantitative theory showing that for some statistical models which allow for discontinuities in the object to be recovered, there are simple algorithms based on the shrinkage of curveletbiorthogonal decompositions, which achieve optimal statistical rates of convergence; that is, such that there are no other estimating procedure which, in an asymptotic sense, give fundamentally better MSEs .

B. Wavelet Domain BivaShrink Denoising Model

Suppose the original image $f(i, j)$ is polluted by noise $n(i, j)$ with variance σ_n , where

$n(i,j) \in N(0,\sigma_n^2)$. And the noisy image is transformed by wavelet. Assume the converted coefficients to be $(a_1(i,j), c_l^k(i,j))$ ($k = 1,2,3$), which respectively denote the horizontal, vertical and diagonal high-frequency coefficients. In BivaShrink denoising, the hard threshold is replaced by the adaptive shrinkage factor to remove the noise of the wavelet coefficients. The aim of denoising is to restore the coefficients $x_l^k(i,j)$ of unpolluted image from the coefficients $c_l^k(i,j)$ of noisy image. Assume the shrinkage factor of coefficient $c_l^k(i,j)$ is $\xi(i,j)$. The estimated value of can be obtained by

$$x_l^k(i,j) = \xi(i,j) \times c_l^k(i,j) \quad (1)$$

In the BivaShrink denoising model[7], the shrinkage factor $\xi(i,j)$ is expressed as (2) for the wavelet coefficient $c_l^{(k)}(i,j)$,

$$\xi(i,j) = \frac{\left(\sqrt{[c_{l+1}^k(i/2, j/2)]^2 + [c_l^k(i,j)]^2} - \frac{3\sigma_n^2}{\sigma_X}\right)_+}{\sqrt{[c_{l+1}^k(i/2, j/2)]^2 + [c_l^k(i,j)]^2}} \quad (2)$$

In (2), the function $(x)_+$ indicates

$$(x)_+ = \begin{cases} x, x > 0 \\ 0, x \le 0 \end{cases}; \ c_{l+1}^k(i/2, j/2)$$

denotes the parent-layer coefficient corresponding to $c_l^k(i,j)$; $\sigma_n = \frac{Median(|c(i,j)|)}{0.6745}$,where $c(i,j) \in HH_1$, and HH_1 is the first-layer high-frequency coefficient after wavelet decomposition;

$$\sigma_X(i,j) = \max\{0, \frac{1}{M} \sum_{(m,n)\in N(i,j)} [c_l^k(i.j)]^2 - \sigma_n^2\} \quad (3)$$

Where $N[i,j]$ represents a neighborhood window of coefficient $c_l^k(i,j)$, and M is total number of coefficients in $N[i,j]$.

C. Improved Estimation of Variance $\sigma_X(i,j)$ in Curvelet Domain

If we assume that the speckle is fully developed, the model of the multiplicatively corrupted backscattered signal can be expressed as

$$g(n) = f(n) \cdot u'(n) = f(n) + f(n) \cdot [u'(n) - 1]$$
$$= f(n) + f(n) \cdot u(n) = f(n) + v(n)$$

in which $g(n)$ and $f(n)$ are the observed noisy signal and the noise-free reflectance, respectively, at pixel position n, and u' is the fading variable modeled as a stationary random process independent of f , with $E[u'(n)] = 1$. The random process $u(n) = u'(n) - 1$ is zero-mean, with variance σ_u^2 and known autocorrelation function . The term $v(n) = f(n) \cdot u(n)$ represents an additive zero-mean signal-dependent noise term, which is proportional to the signal to be estimated. Since $f(n)$ is nonstationary in general, the noise $v(n)$ will be nonstationary as well.

In order to better estimate the variance σ_X of the original image, the proposed method uses the region segmentation to adaptively decide the shape and size of the neighborhood window, and calculates σ_X through intra and inter-layer information. The detailed program is as follows:

(1) Region segmentation. Assume $N(i,j)$ is a neighborhood with $c_l^k(i,j)$ as its center, and $c_{l-1}^k(i^0, j^0)$ is the parent-layer coefficient corresponding of $c_l^k(i,j)$, and $N^0[i^0, j^0]$ is a neighborhood taking $c_{l+1}^k(i^0, j^0)$ as the center. From the literature[10], it is known that $N(i,j)$ can be decomposed into several small subregions $r_0[i,j]$, $r_1[i,j]$, … , $r_{Q-1}[i,j]$, where $r_m[i,j] \cap r_n[i,j] = \Phi$, ($m \neq n$) , or $r_m[i,j] = N[i,j]$, $m = 0,1,\cdots,Q-1$. Only the subregion $r_0[i,j]$ includes the central coefficient $c_l^k(i,j)$.

(2) Calculation of the variance homogeneous measurement(VHM). After the neighborhood $N[i,j]$ of coefficient $c_l^k(i,j)$ is decomposed[11-14], $VHM_m(i,j)$ of the mth subregion is defined as: $VHM_m(i,j) = |\sigma_m^2 - \sigma_0^2|$ where $m = 0,1,\cdots,Q-1$ and $\sigma_m^2(i,j)$ is the variance of local region $r_m[i,j]$. $\sigma_m^2(i,j)$ can be approximately computed through the following equation:

$$\sigma_m^2(i,j) = \frac{1}{M}(c_i^k(m,n))^2$$

where M is the total number of coefficients in region $r_m[i,j]$. $VHM_m(i,j)$ denotes the degree of consistency between $\sigma_m^2(i,j)$ and $\sigma_0^2(i,j)$.

(3) Selection of subregions. According to the decomposition method of $N(i,j)$, decompose parent-layer region $N^0[i^0, j^0]$ into several small subregions $r_0^0[i^0, j^0]$, $r_1^0[i^0, j^0]$, …, $r_{P-1}^0[i^0, j^0]$, and compute $VHM_m^0(i,j)$ between each subregion and $r_0[i,j]$. And then respectively select H and H^0 subregions with the minimal VHM from $r_m[i,j]$ and $r_m^0[i,j]$. Merge H subregions of sublayer in original order, and get a variance estimation region of the sublayer. Similarily, H^0 subregions $r_m^0[i,j]$ of parent layer are merged into a variance estimation region in original order. The merged two regions are the local adaptive window $B[i,j]$ of variance estimation[15-20].

(4) Determine the value of H and H^0. In order to reduce the computational complexity of the experiment, assume both $N(i,j)$ and $N^0[i^0, j^0]$ to be an 9×9 square region which respectively centers on $c_l^k(i,j)$ and

$c_{l+1}^{k}(i^0, j^0)$. $N(i, j)$ and $N^0[i^0, j^0]$ are both decomposed into 9 subregions of 3×3 . Define the regional energy ratio of $N[i, j]$ to be: $K_E(i, j) = \dfrac{\sigma_0^2(i, j)}{\sum_{m=1}^{9}\sigma_m^2(i, j)}$. The experimental results show that if the value of H and H^0 are set according to the following rules, a good denoising effect can be obtained.

$$H = \begin{cases} 4, & K_E \geq 0.5 \\ 5, & K_E < 0.5 \end{cases}; \quad H^0 = H - 1 \qquad (4)$$

After the above four steps, the proper subregions are selected[21-24]. And then they are fused into an adaptive window $B[i, j]$. The $\sigma_X(i, j)$ of the $B[i, j]$ is computed according to formula (3).

D. Improved Denoising Method based on Curvelet Domain BivaShrink Model

After $\sigma_X(i, j)$ is obtained, the noise of the image can be removed according to formula(2). The steps of SAR image denoising are as follows:

(1) Curvelet transform of the noisy image.

(2) Determine the local adaptive window $B[i, j]$ according to VHM for the high-frequency curvelet coefficients of different scales.

(3) Compute the variance $\sigma_X(i, j)$ of the original image according to formula (3). The noise variance σ_n is obtained through the median estimation, that is $\sigma_n = \dfrac{Median(|c(i, j)|)}{0.6745}$, where $c(i, j) \in HH_1$.

(4) Remove noise according to formula (1) for the curvelet coefficients of different scales.

(5) Curvelet inverse transform for the denoised coefficients and get the denoised image.

III. SIMULATION EXPERIMENT AND ANALYSIS

This paper uses the following three criteria to objectively evaluate the denoising effect of SAR image[1,9]：Equivalent number of looks(ENL); Mean of ratio image(MR); Edge saving index (ESI). In the experiment, we respectively use the BivaShrink wavelet denoising(BSW), the hard-threshold curvelet denoising(HTC) and our denoising method to remove the speckle noise of two test images from American sandia national laboratory, which are the X-SAR images of 512×512 size. Fig.1 and Fig.2 are respectively the denoised results of the two images through the different methods. Table1, Table2 and Table3 are the evaluation standards of the different methods. Assume the number of layers of wavelet decomposition and curvelet decomposition to be 4. In order to quantitatively compare denoising effect of all methods, we respectively select three homogeneous regions from Fig.1(a) and Fig.2(a).

TABLE I.

ENL OF THE SELECTED REGIONS

	SAR Image 1			SAR Image 2		
	Region 1	Region 2	Region 3	Region 1	Region 2	Region3
Original Image	2.784	4.226	2.855	9.424	9.155	9.914
BSW	27.532	60.233	33.162	54.879	42.753	57.461
HTC	42.758	71.391	98.526	91.433	87.366	109.822
The Proposed Method	61.250	90.442	107.341	121.462	115.129	141.377

TABLE II.

MR AND ESI OF SAR IMAGE 1

		ESI	
	MR	Horizontal	Vertical
BSW	1.320	0.4268	0.4752
HTC	1.127	0.4987	0.5521
The Proposed Method	1.063	0.5694	0.6237
Ideal	1.000	1.0000	1.0000

TABLE III.

MR AND ESI OF IMAGE 2

		ESI	
	MR	Horizontal	Vertical
BSW	1.293	0.5447	0.5461
HTC	1.107	0.6157	0.6042
The Proposed Method	1.018	0.6586	0.6558
Ideal	1.000	1.0000	1.0000

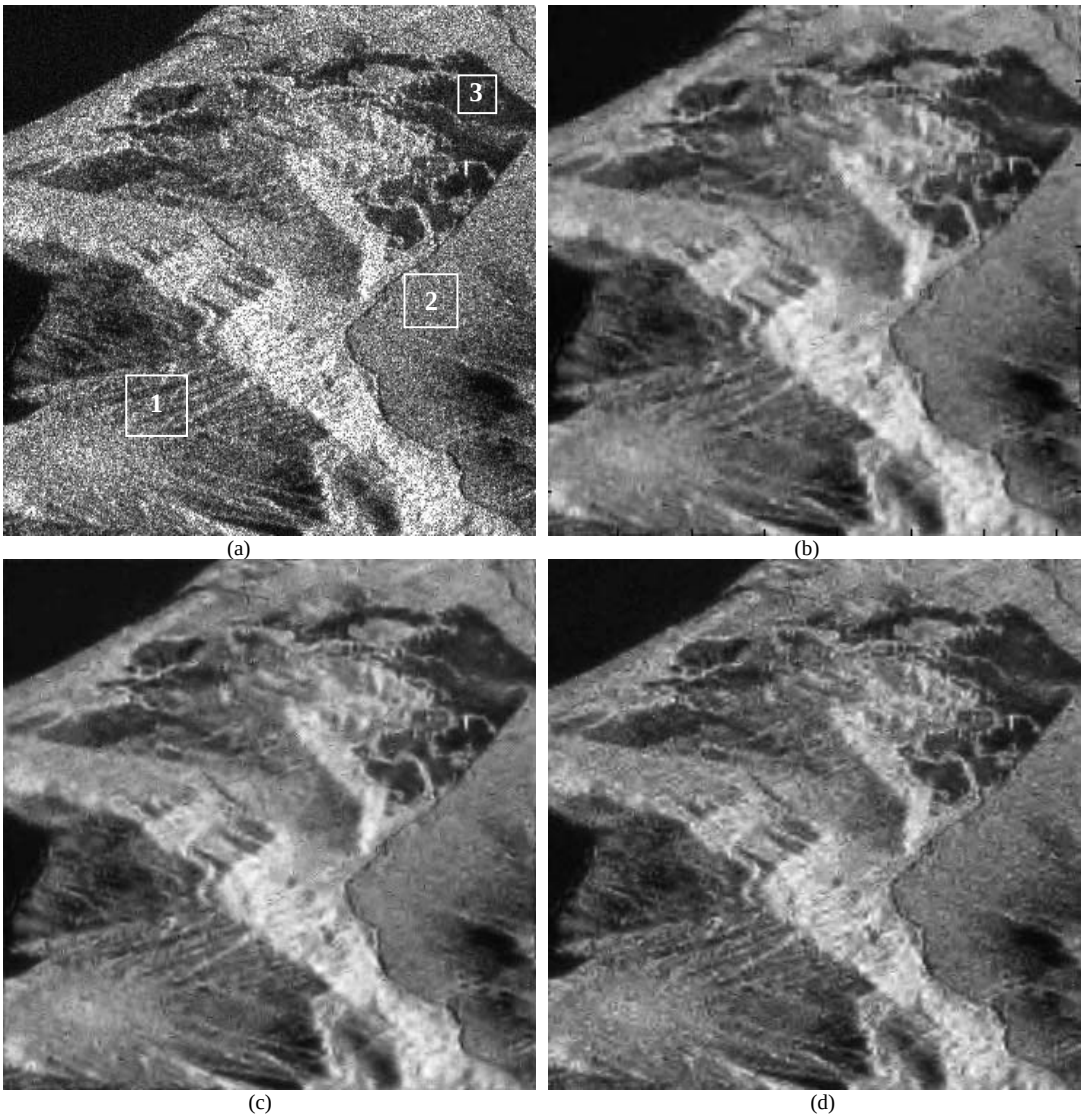

Figure 1. Experimental results of SAR image 1 (a) original SAR image, (b) BSW, (c) HTC , (d) The proposed method

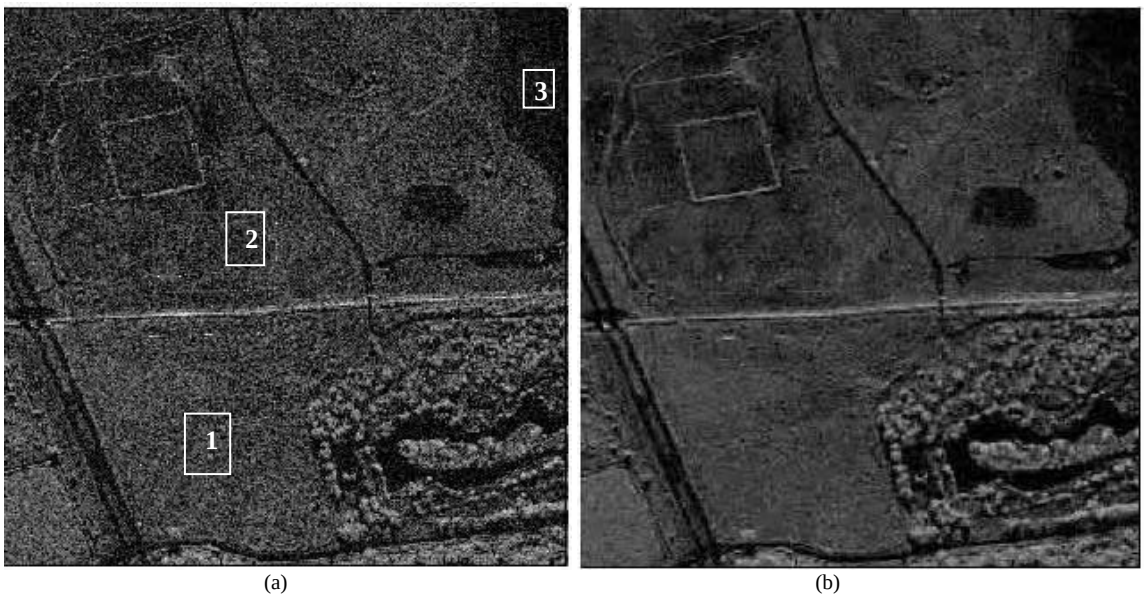

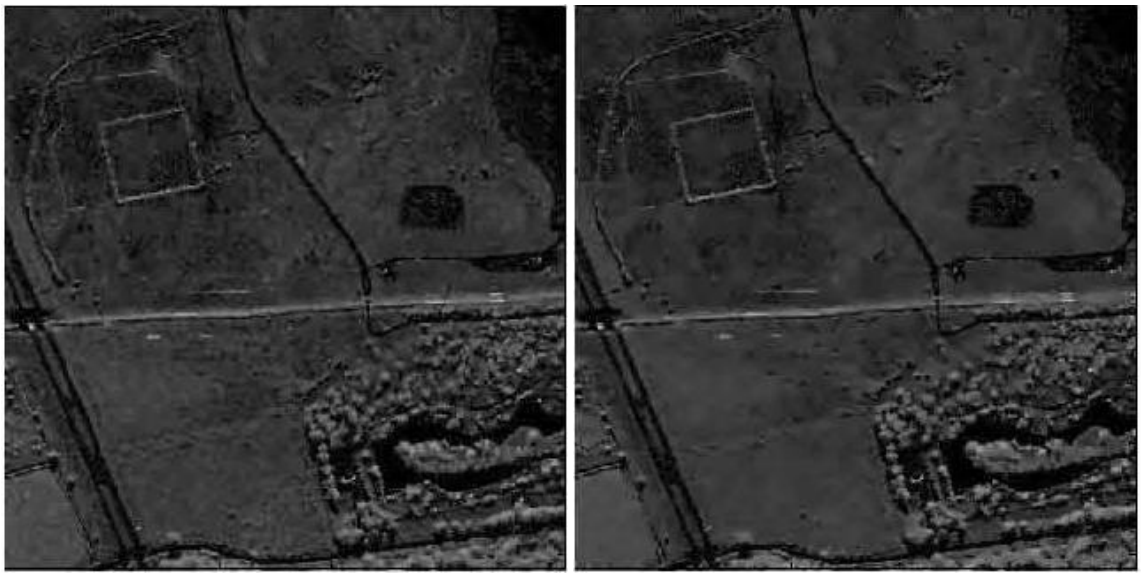

(c) (d)

Figure 2. Experimental results of SAR image 2 , (a) Original SAR image, (b) BSW, (c) HTC, (d) The proposed method

The sizes of the selected regions in Fig.1(a) are respectively 25×25,35×35,50×50. Similarly, the sizes in Fig.2(a) are respectively 56×90、45×70、25×35.

The data in Table1 reveals the proposed method can suppress the speckle of homogeneous region better than the others. Compared with BSW and HTC, the ENL value of the proposed method respectively average improves about 60.164 and 22.623. Furthermore, Table2 and Table3 respectively denote the value of MR and ESI. The data shows that the proposed method has the optimal MR and ESI. Its value of MR respectively is less about 0.136 and 0.076 than that of the others. Its value of ESI is more about 0.1228 than BSW, and more about 0.0567 than HTC. So the proposed method can't only remove noise but also effectively maintain the edges and texture details of image. It can greatly improve the speckle suppression effect in contrast with BSW and HTC.

IV. SUMMARY

An improved SAR image speckle suppression algorithm based on curvelet transform is proposed according to the distribution properties of curvelet coefficients. The method realizes denoising through optimally estimate the threshold shrinkage factor of curvelet coefficients. When calculating $\sigma_X(i,j)$, it firstly computes the variance homogeneous measurement and the regional energy ratio, so as to adaptively determine the size and shape of neighborhood window. And then it uses the intra and inter-layer information to optimally estimate the value of $\sigma_X(i,j)$. The experimental results show the proposed method is an efficentiv speckle suppression algorithm, which can effectively reduce speckle noise, and better maintain edge and texture details.

ACKNOWLEDGMENT

The research work is supported by the National Natural Science Foundation of China (Grant No. 41071270), LIESMARS Special Research Funding , Natural Science Fund of Hubei Province(2010CDB03305), Wuhan Chenguang Program(201150431096) , State Key Laboratory of Satellite Ocean Enviroment Dynamics Research Funding (Grant No. SOED1102), The Second Institute of Oceanography Research Project: LIDAR bathymetry data processing and key technologies , Open Fund of State Key Laboratory of Information Engineering in Surveying Mapping and Remote Sensing(11R01), Self-determined and Innovative Research Funds of WUT(123210005); the fundamental research funds for the central universities(2012-IV-043).

REFERENCES

[1] Maryam A, Hamidreza A, Alireza M. Speckle suppression in SAR images using the 2-D GARCH model. IEEE Transactions on Image Processing, 18(2009)250-259.

[2] Stian S, Eltoft T. A stationary wavelet-Domain wiener filter for correlated speckle. IEEE Transactions on Geoscience and Remote Sensing, 46(2008), 1219-1230.

[3] Fabruzui A, Tiziano B, Luciano A. Multiresolution MAP despeckling of SAR images based on locally adaprive generalized Gaussian pdf modeling. IEEE Transactions on Image Processing, 15(2006)3385-3399.

[4] Foucher S, Benie G B, Boucher J M. Multiscale MAP filtering of SAR images. IEEE Transactions on Image Processing, 10(2001)49-60.

[5] Donoho D L. Orthonormal ridgelets and linear singularities. SIAM Journal on Mathematical Analysis, 31(2000)1062-1099.

[6] Strack J L, Candes E I, Donoho D I. The Curvelet transform for image denoising. IEEE Trans on Image Processing, 11(2002)670-684.

[7] Sendur, Selesnick I W. Bivariate Shrinkage Functions for Wavelet based Denoising Exploiting Interscale Dependency. IEEE Transactions on Signal Processing, 50(2002)2744-2756.

[8] Cheng Lizhi, Wang Hongxia, Luo Yong. The Theory and Application of Wavelet. Science Press, Beijing, 2004.
[9] Marko H, Dusan G, Zarko C. Autobinomial model for SAR image despeckling and information extraction. IEEE Transactions on Geoscience and Remote Sensing, 47(2009)2818-2835..
[10] Han Chao, zhang Bichao, Zhang zhidong, etc. Synchronization control system of guide seat lifting scaffold. Journal of Xi'an Polytechnic University, 2011, 25(6):857-866.
[11] Luo Peng. Denoising method of image based on undecimated curvelet transform. Journal of North University of China (Natural Science Edition), 2011, 32(3):348-354.
[12] Xu Weiling, Shen Minfen, Fang Ruoyu. Speckle reduction for SAR image using edge directions in complex wavelet domain. Signal Processing, 2011, 27(8): 1179-1183.
[13] Fan Qiuyue, zhang Anfa. SAR image filtering based on biorthogonal wavelet transform. Communications Technology, 2010, 43(8): 192-194.
[14] Liu Shuaiqi, Hu Shaohai, Xiao Yang. SAR image de-noised based on wavelet-contourlet transform with cycle spinning. Signal Processing, 2011, 27(6): 837-842.
[15] Li Min, Zhang Ziyou, Lu Linju. Speckle reduction of SAR image based on morphological Haar wavelet. Journal of Computer Applications, 2012, 32(3):746-748.
[16] Liu Jun, Li Deren, Shao Zhenfeng. Fusion of remote sensing images based on fast discrete Curvelet transform. Geomatics and Informations Science of Wuhan University, 2011, 36(3):333-337.
[17] Zhang Shuangxi, Zhang Lei, Guo Rui, etc. SAR interference suppression algorithm for narrow band interference via wavelets. Journal of XiDian University, 2011, 38(5):108-114.
[18] Dong Lieqian, Li Zhenchun, Wang Deying, etc. Ground-roll suppression based on the second generation curvelet transform. Oil Geophysical Prospecting, 2011, 46(6); 897-904.
[19] Li Xin, Zhang Wenmao, Zeng Qinlin. Study on speckle noise filter in the ESPI image based on curvelet transform. Laser & Infrared, 2011, 41(9): 1045-1048.
[20] Liu Guochang, Chend Xiaohong, Guo Zhifeng, Missing seismic data rebuilding by interpolation based on curvelet transform. Oil Geophysical Prospecting, 2011,46(2): 237-246.
[21] Xue Nian, Zhou Lixia, Yin Zhongke. Curvelet thresholding for seismic data denoising and interpolating. Journal of Transportation Engineering and Information, 9(2):86-91.
[22] Jinrong Hu, Yifei Pu, Jiliu Zhou. A Novel Image Denoising Algorithm Based on Riemann-Liouville Definition. Journal of Computers, 6(7), 2011, 1332-1338.
[23] Beiji Zou, Haoyu Zhou, Hao Chen, Cao Shi. Multi-Channel Image Noise Filter based on PCNN. Journal of Computers, 7 (2), 2012, 475-482.
[24] Zhe Liu, Xiaoxian Zhen, Cong Ma. A Novel Image Reconstruction Algorithm Based on Concatenated Dictionary. Journal of Computers, 7(2012)444-449.

Wang Wenbo received the Ph.D. degree in mathematical physics from the School of Mathematics and Statistics, Wuhan University, in 2006.

From 2006 to 2012, he worked successively at the College of Science, Wuhan University of Science and Technology, China., where currently he is the Chief Scientist of the Computational Sciences and Engineering Division.

His research interests include mathematical modeling, analysis and optimal control of partial differential equations, dynamical systems, inverse problems, global optimization, and quantum information science. He has served as an Associate Editor for the Acta Geodaetica et Cartographica Sinica, and Signal Processing.

Zhang Xiaodong received the Ph.D. degree in State Key Laboratory of Information Engineering in Surveying, mapping and Remote Sensing, in 2005.

From 1999 to 2012, he worked successively at the State Key Laboratory of Information Engineering in Surveying, mapping and Remote Sensing, Wuhan University, China. where currently he is the remote sensing image processing and application.

His research interests include mathematical modeling, analysis and wavelet analysis theory and application in remote sensing images processing, and the change detection of SAR.

Wang Xiangli received the Ph.D. degree in Electrical and Computer Engineering from the School of Computer Science and Technology, Wuhan University of Technology, in 2011.

From 2000 to 2012, she worked successively at the School of Computer Science and Technology, Wuhan University of Technology, China, where currently he is the remote sensing image processing and application.

His research interests include mathematical modeling, analysis and wavelet analysis theory and application in remote sensing images processing, and the change detection of SAR.